ACS APPLIED MATERIALS & INTERFACES

Research Article

www.acsami.org

Superwetting Double-Layer Polyester Materials for Effective Removal of Both Insoluble Oils and Soluble Dyes in Water

Bucheng Li,[†] Lei Wu,[†,‡] Lingxiao Li,[†] Stefan Seeger,[§] Junping Zhang,*[,†] and Aiqin Wang[†]

[†]Center of Eco-material and Green Chemistry, Lanzhou Institute of Chemical Physics, Chinese Academy of Sciences, Lanzhou, 730000, P. R. China

[‡]Graduate University of the Chinese Academy of Sciences, Beijing, 100049, P. R. China

[§]Department of Chemistry, University of Zurich, Zurich, 8057, Switzerland

Supporting Information

ABSTRACT: Inspired by the mussel adhesive protein and the lotus leaf, Ag-based double-layer polyester (DL-PET) textiles were fabricated for effective removal of organic pollutants in water. The DL-PET textiles are composed of a top superamphiphilic layer and a bottom superhydrophobic/superoleophilic layer. First, the PET textiles were modified with a layer of polydopamine (PDA) and deposited with Ag nanoparticles to form the PET@PDA@Ag textiles. The top superamphiphilic layer, formed by immobilizing Ag_3PO_4 nanoparticles on the PET@PDA@Ag textile, shows excellent visible-light photocatalytic activity. The bottom superhydrophobic/superoleophilic layer, formed by modifying the PET@PDA@Ag textile using dodecyl mercaptan, is mechanically, environmentally, and chemically very stable. The water-insoluble oils with low surface tension can penetrate both layers of the DL-PET textiles, while the water with soluble organic dyes can only selectively wet the top layer owing to their unique wettability. Consequently, the water-soluble organic contaminants in the collected water can be decomposed by the Ag_3PO_4 nanoparticles of the top layer under visible-light irradiation or even sunlight in room conditions. Thus, the DL-PET textiles can remove various kinds of organic pollutants in water including both insoluble oils and soluble dyes. The DL-PET textiles feature unique wettability, high oil/water separation efficiency, and visible-light photocatalytic activity.

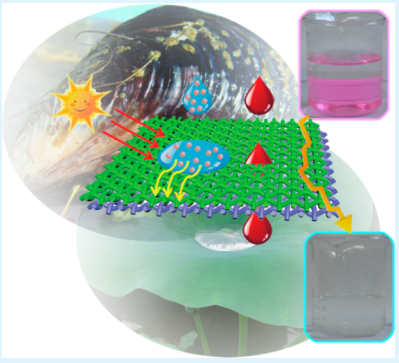

KEYWORDS: *bioinspiration, superhydrophobic, Ag, photocatalysis, water purification*

INTRODUCTION

Nowadays, water pollution has become a serious problem accompanying rapid development of the economy, especially in developing countries including China, India, and Zambia.[1,2] Water pollution has great adverse effects on the environment and human health.[3] Water pollution causes approximately 14 000 deaths per day. Organic pollutants including insoluble oils and soluble dyes are a main kind of contaminant in water.[3,4] Various approaches, e.g., oil/water separation, photocatalyzed decomposition, and adsorption, have been used to purify water.[5−8]

Recently, superwetting materials including mesh/membrane, sponge, carbon nanotubes, macroporous gels, and polymer gels[9−19] have been proven to be very promising in selective removal of water-insoluble oils from water owing to their superior oil/water selectivity to traditional materials such as clay and activated carbon. Li et al. prepared a superhydrophobic sponge with high oil absorbency using a conjugated polymer.[20,21] Tuteja et al. fabricated superhydrophilic/superoleophobic hygro-responsive membranes for efficient oil/water separation.[22] Jiang et al. used superhydrophilic and underwater superoleophobic materials for selective oil/water separation and oil capture.[23,24] Inspired by the conical cactus spines, they also designed oleophilic cone arrays for continuous collection of micrometer-sized oil droplets in water.[25] However, these superwetting materials cannot remove water-soluble organic contaminants, e.g., the frequently encountered organic dyes.

Ag_3PO_4 nanoparticles (Ag_3PO_4−NPs) are a kind of newly discovered semiconductor photocatalyst which can split water and decompose dyes under visible-light irradiation.[26] Ag_3PO_4−NPs exhibit extremely high photooxidative capability for O_2 evolution from water with a quantum efficiency of up to 90% at $\lambda > 420$ nm, which is significantly higher than the previously reported values. However, use of photocatalysts in the form of NPs in purifying water may cause secondary pollution. It is an important task of general interest to control the environmental and health hazards of photocatalyst nanoparticles.[27] Immobilization of Ag_3PO_4−NPs on substrates should be an elegant solution to solve the problem. Compared with the developed strategies for immobilization of TiO_2−NPs,[28] immobilization of Ag_3PO_4−NPs is still a gap to be filled. In addition, oils must be

Received: April 17, 2014
Accepted: June 23, 2014
Published: June 23, 2014

separated from polluted water before being treated by Ag_3PO_4 in order to fully exhibit the efficiency of photocatalysis.

Here we report fabrication of double-layer Ag-based superwetting polyester (DL-PET) textiles which can remove both insoluble oils and soluble dyes in water under visible-light irradiation as inspired by the mussel adhesive protein and the lotus leaf. DL-PET textiles are composed of a top super-amphiphilic layer with immobilized Ag_3PO_4−NPs and a bottom superhydrophobic/superoleophilic layer. The water-insoluble oils with low surface tension can penetrate both layers of the DL-PET textiles, while water with soluble organic dyes can only selectively wet the top layer owing to their unique wettability. The water-soluble organic contaminants in the collected water can be decomposed by the Ag_3PO_4−NPs of the top layer under visible-light irradiation or even sunlight. DL-PET textiles feature unique wettability, high oil/water separation efficiency, and visible-light photocatalytic activity.

EXPERIMENTAL SECTION

Materials. The fluorinated PET textiles were supplied by HM Group, China. Dopamine hydrochloride (98%) was purchased from Shanghai DEMO Medical Tech Co., Ltd., China. Tris-(hydroxymethyl)amino methane hydrochloride (Tris-HCl), $AgNO_3$, $NH_3{\cdot}H_2O$, *n*-butylamine, anhydrous ethanol, $Na_2HPO_4{\cdot}12H_2O$, dodecyl mercaptan (DM), *n*-octane, rhodamine B (RhB), and methylene blue (MB) were purchased from China National Medicines Co., Ltd. All chemicals were used as received without further purification.

Fabrication of PET@PDA Textiles. Dopamine (1.5 mg/mL) was dissolved in 10 mM Tris-HCl, and the pH was adjusted to 8.5 using 1 M NaOH. A piece of 5 × 5 cm PET textile was added to 60 mL of the above dopamine solution. The solution was mechanically stirred for 24 h at 25 °C. Then, the PET@PDA textile was washed by deionized water several times and dried in an oven at 60 °C.

Fabrication of PET@PDA@Ag Textiles. $AgNO_3$ (0.68 mg/mL) was dissolved in anhydrous ethanol under vigorous stirring in a conical flask. A piece of the PET@PDA textile was immersed in the $AgNO_3$ solution. Then, 10 mL of *n*-butylamine solution (10 mM in ethanol) was added to the $AgNO_3$ solution at 50 °C. The conical flask was shaken in a thermostatic shaker (THZ-98A, Chincan, Zhejiang, China) at 50 °C and 120 rpm for 1 h to form the PET@PDA@Ag textile. The PET@PDA@Ag textile was washed with ethanol several times and dried in an oven at 60 °C.

Fabrication of PET@PDA@Ag@DM Textiles. A piece of the PET@PDA@Ag textile was immersed in the DM ethanol solution (2% v/v) at room temperature for 24 h. The sample was washed with ethanol several times and dried in a vacuum oven at 60 °C.

Fabrication of PET@PDA@Ag@Ag_3PO_4 Textiles. PET@PDA@Ag@Ag_3PO_4 textiles were prepared using silver−ammino ($[Ag(NH_3)_2]^+$) complex as the silver ions source. In a typical synthesis, $AgNO_3$ (0.17 g) was dissolved in 10 mL of water in a conical flask. Ammonia aqueous solution (0.3 M) was added drop by drop to the above solution to form a transparent solution. Then, a piece of the PET@PDA@Ag textile was immersed in the $[Ag(NH_3)_2]^+$ complex solution for 10 min. Subsequently, the Na_2HPO_4 aqueous solution (0.15 M) was added into the solution to form Ag_3PO_4 submicrocubes on the surface of the textile. PET@PDA@Ag@Ag_3PO_4 textile was washed with deionized water several times and dried in a vacuum oven at 40 °C.

Measurement of Water Shedding Angle (WSA). Owing to the fact that the surfaces of some substrates such as textile and sponge are macroscopically rough, it is very difficult to detect the full drop profile for contact angle (CA) measurement (Figure S1, Supporting Information). Consequently, the classical CA measurement, highly dependent on the method of drop shape analysis, is unsuited to reliably evaluate the wetting properties of the surfaces. Thus, WSA is used instead of CA and sliding angle according to a previous reported method (Figure S2, Supporting Information).[29,30] Typically, the samples were fixed onto a glass slide and placed on the tilting table of the Contact Angle System OCA 20 (Dataphysics, Germany). A syringe was mounted above the tilting table with a fixed needle to a substrate distance of 10 mm. The syringe was positioned in a way that a drop falling from the needle would contact the substrate 8 mm from the bottom end of the sample. The needle with an inner diameter of 110 μm was used to produce liquid droplets with a volume of 7 ± 0.3 μL. To determine the WSA, measurements were started at an inclination angle of 50°. Droplets of liquid were released onto the sample at a minimum of three different positions. If all drops completely bounced or rolled down the sample, the inclination angle was reduced by 2°, and the procedure was repeated until one or more of the droplets would not completely roll down the surface. The lowest inclination angle at which all drops completely rolled down or bounced off the surface was noted as the WSA.

Stability Tests. Abrasion tests were performed according to a previously reported method (Figure S3, Supporting Information).[31] The sample was fixed onto the stainless steel column and moved repeatedly (40 cm for one cycle) on the abrasion partner at 5 kPa. In order to simulate the authentic utilization, the abrasion tests were performed using sandpaper (2000 meshes) as the abrasion partner. The WSAs after 10, 25, 50, 75, and 100 cycles of abrasion were recorded. Before WSA measurement, the samples were first washed with ethanol and then dried at 60 °C because a lot of sands penetrated into the samples during the test. For the laundering durability tests, samples were washed without detergent in a washing machine with 10 pieces of cotton textiles (20 × 20 cm) for 10 cycles (30 min each) at room temperature. After each washing cycle, the sample was washed in turn with deionized water and absolute ethanol three times and then dried in an oven at 60 °C before WSA measurement.

Oil/Water Separation. For oil/water separation, a mixture of 10 mL of oil and 30 mL of RhB aqueous solution (1 ppm) was poured slowly into the custom-built setup. The DL-PET textile was fixed between a glass tube and a flask. Once poured into the custom-built setup, oils with high density will sink to the bottom and penetrate the textile. Oils with low density contact the textile before water when the mixture is slowly pulled into the custom-built setup because of their lower density than water. The water concentration in the separated oil was determined using a C20 Compact Karl Fischer Coulometer (Mettler Toledo, Switzerland). The oil concentration in the separated water was measured using an Aurora 1030w Total Organic Carbon Analyzer (O-I-Analytical, USA).

Photocatalytic Reactions. The sample was put in a solution of RhB (1 ppm, 100 mL) or MB (5 ppm, 100 mL), which was then irradiated with a 300W Xe arc lamp equipped with an ultraviolet cutoff filter to provide visible light with $\lambda \geq 420$ nm. Degradation of dyes was monitored using a UV−vis spectrophotometer (Specord 200, Analytik Jena AG). For the recycling experiments, the sample was taken out of the RhB solution after every run of photocatalytic reaction, washed with deionized water, and dried under a N_2 flow. Then the sample was put in a fresh RhB solution for the next run of reaction.

Characterization. The micrographs of the samples were taken using a field emission scanning electron microscope (SEM, JSM-6701F, JEOL). Before SEM observation, all samples were fixed on aluminum stubs and coated with gold (~7 nm). X-ray photoelectron spectra (XPS) were obtained using a VG ESCALAB 250 Xi spectrometer equipped with a monochromated Al Kα X-ray radiation source and a hemispherical electron analyzer. Spectra were recorded in the constant pass energy mode with a value of 100 eV, and all binding energies were calibrated using the C 1s peak at 284.6 eV as the reference. Powder X-ray diffraction (XRD) analysis was performed using a diffractometer with Cu anode (PAN alytical X'pert PRO), running at 40 kV and 30 mA, scanning at 3°/min. All tests were carried out in triplicate. The high-speed video was taken using the Contact Angle System OCA 20 at 400 fps.

RESULTS AND DISCUSSION

Design of DL-PET Textiles. Mimicking the adhesive proteins of mussels, Messersmith et al. demonstrated that

dopamine could polymerize and deposit on all kinds of substrates.[32] The as-formed polydopamine (PDA) is of chemical versatility and can be used as a platform for diverse secondary reactions.[33] The PET textiles, used as the substrates in this study, are modified with a thin layer of PDA to form PET@PDA and then deposited with Ag−NPs to form PET@PDA@Ag (Scheme 1). On one hand, the PET@PDA@Ag textiles can be converted to the superhydrophobic/superoleophilic bottom layer, PET@PDA@Ag@DM, by decreasing the surface tension using DM. On the other hand, the PET@PDA@Ag textiles can be used for immobilization of Ag_3PO_4−NPs to form the superamphiphilic top layer, PET@PDA@Ag@Ag_3PO_4, of the DL-PET textiles. DL-PET textiles are formed simply by combining the PET@PDA@Ag@Ag_3PO_4 (top) and PET@PDA@Ag@DM (bottom) textiles. Polluted water containing insoluble oils and soluble dyes can be easily purified by the DL-PET textiles according to the following procedure. First, the polluted water is poured onto the DL-PET textiles. Oil quickly penetrates both layers of the DL-PET textiles, but water with soluble dyes is stopped by the bottom PET@PDA@Ag@DM layer. Subsequently, the dyes in the collected water are gradually decomposed under visible-light irradiation, and purified water is obtained.

Scheme 1. Preparation of PET@PDA, PET@PDA@Ag, PET@PDA@Ag@DM, PET@PDA@Ag@Ag_3PO_4, and DL-PET Textiles, and the Water Purification Process Using the DL-PET Textiles

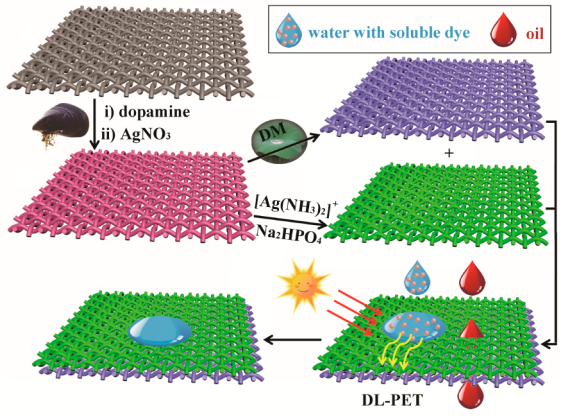

PET@PDA@Ag Textiles. In pH 8.5 Tris-HCl buffer solution, dopamine spontaneously polymerized and deposited on the fibers of the PET textiles. The white PET textiles become brown PET@PDA with a PDA layer thickness of about 20 nm (Figure S4a and S4b, Supporting Information). The smooth surface of the PET fibers becomes rough, and a lot of PDA-NPs can be seen after being modified with dopamine (Figures 1a, 1b, and S5, Supporting Information). In the XPS spectrum of PET@PDA (Figure 1d), the new N 1s peak at 400 eV attributed to PDA appears and the F 1s peak of PET becomes very weak, which also indicate that the PET fibers are covered with a layer of PDA. Deposition of PDA also results in an evident change in the wettability (Figure 1e; Movie S1, Supporting Information, parts 1 and 2). The hydrophobic PET textile with a CA_{water} of 137.1° ± 10.8° becomes superhydrophilic (CA_{water} = 0°). Water drops could easily wet and penetrate the PET@PDA textiles in ∼1.3 s. The superhydrophilic PET@PDA textiles become hydrophobic (CA_{water} = 125.6° ± 12.2°) and darker after deposition of the Ag−NPs by reduction with *n*-butylamine in ethanol (Figures 1e and S4c; Movie S1, Supporting Information, part 3).[34] The CA_{water} is 125.6° ± 12.2° on the whole PET@PDA@Ag textile and cannot roll off even turned upside down, indicating that the textile is uniformly coated with the Ag−NPs. The dense and uniform layer of Ag−NPs on the surface of the PET@PDA fibers can be seen directly from the digital and SEM images (Figures 1c and S6, Supporting Information). Deposition of Ag−NPs is also confirmed by the appearance of Ag peaks in the XPS spectrum of PET@PDA@Ag (Figure 1d). The C 1s, N 1s,

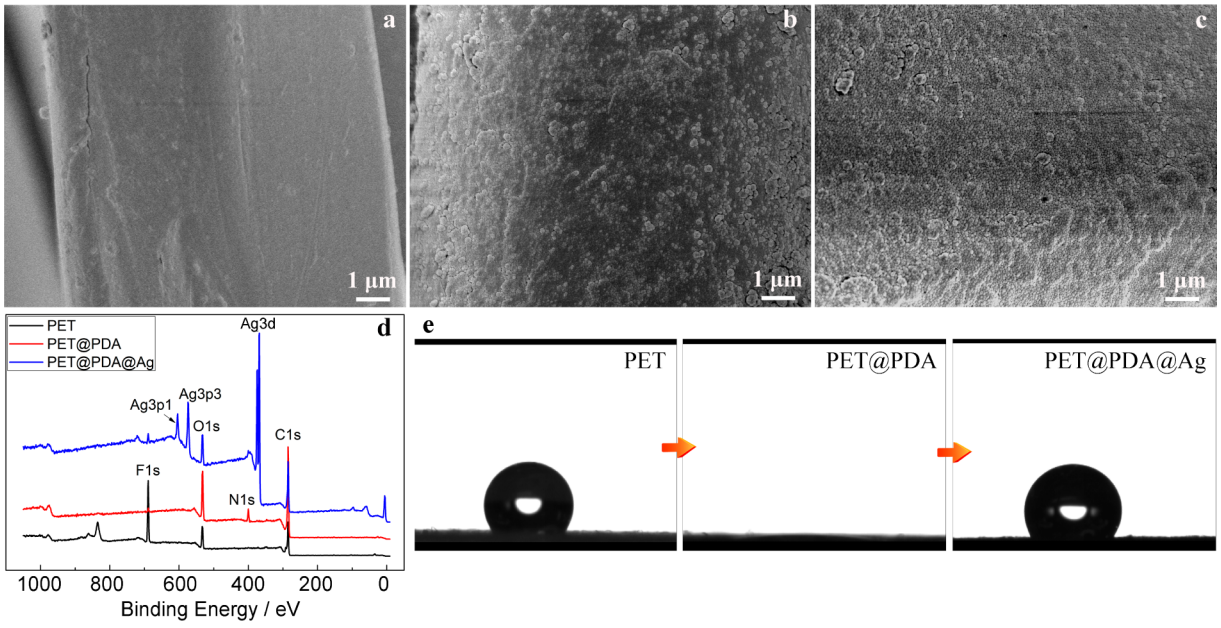

Figure 1. SEM images of (a) PET, (b) PET@PDA, (c) PET@PDA@Ag, and (d) their XPS spectra. (e) Images of water drops on PET, PET@PDA, and PET@PDA@Ag textiles.

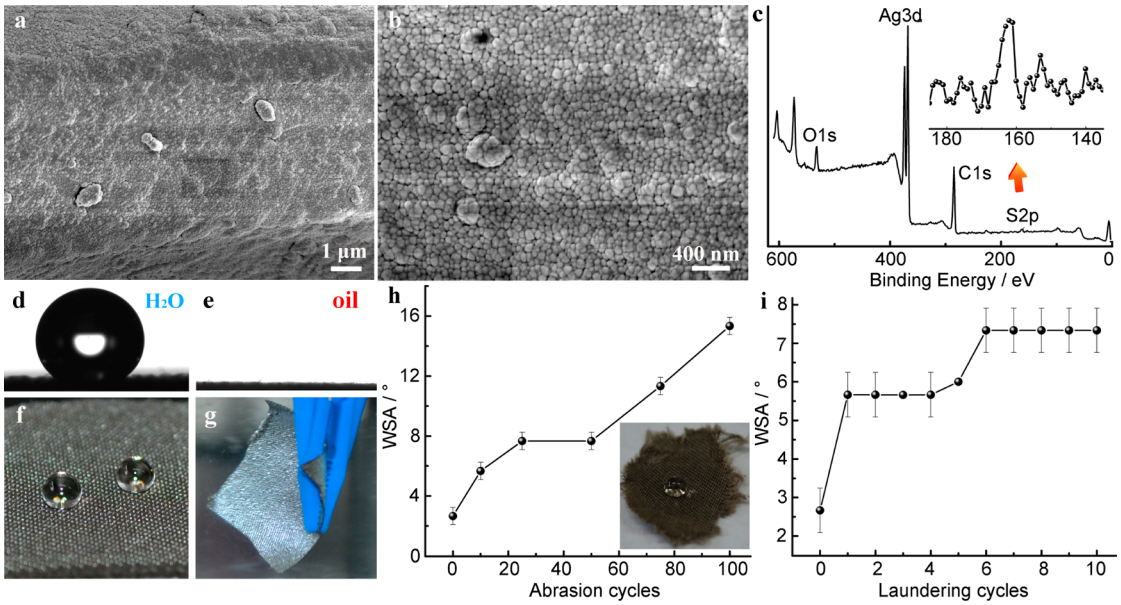

Figure 2. (a, b) SEM images and (c) XPS spectrum of PET@PDA@Ag@DM. Images of (d) water, (e) oil and (f) water drops on PET@PDA@Ag@DM, and (g) PET@PDA@Ag@DM immersed in water. WSA (10 μL) changes of PET@PDA@Ag@DM depending on (h) abrasion and (i) laundering cycles (30 min each).The insert in (h) is the image of PET@PDA@Ag@DM with water drop on it after 100 abrasion cycles.

and F 1s peaks of PET@PDA become weaker after being coated with the Ag−NPs.

PET@PDA@Ag@DM Textiles. The superhydrophobic/superoleophilic bottom layer was produced by modifying the hierarchical PET@PDA@Ag textile with an ethanol solution of DM. The surface morphology of PET@PDA@Ag@DM is very similar to that of PET@PDA@Ag (Figure 2a and 2b), indicating monolayer modification with DM. The new S 2s peak at 162.4 eV in the XPS spectrum of PET@PDA@Ag@DM confirms the successful binding of DM on the surface of PET@PDA@Ag (Figure 2c). The PET@PDA@Ag@DM textile is superhydrophobic and superoleophilic owing to the low surface tension of the alkyl chain of DM (Figure 2d−f). Water drops are in the Cassie−Baxter state on the PET@PDA@Ag@DM textile and could easily roll off the slightly tilted surface (~3°), indicating very high superhydrophobicity. The coated textile is reflective in water because of the existence of an air cushion between water and the textile (Figure 2g). The air cushion is stable over 4 weeks, and the textile remains completely dry after being taken out. Moreover, a 7 μL water droplet released from a height of 15 mm (dispensing tip to surface) could bounce many times on the horizontal PET@PDA@Ag@DM textile (Movie S1, Supporting Information, part 4). This means the kinetic energy of the water drop is well conserved by the surface deformation and the dissipation of the kinetic energy by work of adhesion is very low during the impact against the surface.[35] Different from water, the PET@PDA@Ag@DM textile can be easily wetted by oil. Oil drops could wet and penetrate the textile very quickly. The obviously different wettability of the PET@PDA@Ag@DM textile toward water and oil makes it a very promising material for oil/water separation.

The PET@PDA@Ag@DM textiles show excellent mechanical, environmental, and chemical durability owing to the in turn covalent binding of PDA, Ag, and DM on the surface of the PET fibers.

The abrasion resistance of the textiles was evaluated. Although the textiles are seriously damaged after 100 abrasion cycles at 5 kPa using sandpaper as the abrasion partner (insert in Figure 2h), water drops still show very high CA and no obvious change in CA can be detected. However, it is impossible to get an accurate outline of the water drops (Figure S1, Supporting Information) and then measure the CA and CA hysteresis exactly because the textile surface is macroscopically rough, pliant, and nonreflective.[29] Thus, the WSA was used to evaluate the water-repellent properties of the coatings instead of CA and CA hysteresis in this study. The WSA increases gradually from 3° to 16° with increasing abrasion cycles (Figure 2h). Water drops keep nearly spherical in shape and still could easily roll off the tilted residual sample after 100 abrasion cycles.

The laundering durability of the PET@PDA@Ag@DM textiles was also evaluated. A laundering procedure is a combination of various mechanical interactions, such as shearing forces with water and the wall of the container.[36] Only a few papers reported laundering durability of superhydrophobic materials. For example, the CA of the coated cotton fabric decreased to 125° after 5 laundering cycles owing to the cracking of the silica gel film on the fiber surface according to Gao et al.[37] For the PET@PDA@Ag@DM textile in this study, no change in CA can be detected after 10 cycles of machine wash. The WSA increases gradually with increasing laundering cycles and remains below 8° after 10 cycles (Figure 2i), indicating excellent laundering durability of the superhydrophobic coating. A 10 μL water drop could easily bounce off the 10° tilted sample even after 10 laundering cycles. This phenomenon clearly shows the very weak interaction between the washed textile and the water drop.[38]

With respect to the environmental and chemical durability of the superhydrophobic PET@PDA@Ag@DM textiles, a series of experiments has been done under various conditions (Table 1). The coatings are stable against UV irradiation (200−400 nm), 0.1 M HCl solution, 0.1 M NaOH solution, and low and high temperature. No obvious change in WSA was detected after these treatments. The PET@PDA@Ag@DM textiles are also resistant to various organic solvents and oils. The WSA is

Table 1. WSA on the PET@PDA@Ag@DM Textiles after Treatment under Various Conditions for 1 and 24 h

treatments	1 h	24 h
UV, 200−400 nm	2.3 ± 0.6	4.3 ± 0.6
0.1 M HCl	3.3 ± 0.6	5.7 ± 0.6
0.1 M NaOH	4.0 ± 0	6.3 ± 0.6
−30 °C	2.3 ± 0.6	3.3 ± 0.6
150 °C	2.3 ± 0.6	2.3 ± 0.6
ethanol	4.0 ± 0	5.7 ± 0.6
toluene	2.7 ± 0.6	2.7 ± 0.6
acetone	3.0 ± 0	4.7 ± 0.6
petrol	3.0 ± 0	3.0 ± 0
crude oil	3.3 ± 0.6	3.3 ± 0.6

below 7° after being immersed in these organic solvents and oils for 24 h.

As is well known, the low stability of superhydrophobic coatings is the bottleneck we are facing for their practical applications, although thousands of reports in the literature about superhydrophobic coatings can be found.[39] The performance of superhydrophobic materials in selective oil/water separation is closely related to their superhydrophobicity. The superior stability of the superhydrophobic PET@PDA@Ag@DM textiles to most of the reported ones paves the way for their application in selective oil/water separation.

PET@PDA@Ag@Ag_3PO_4 Textiles. The PET@PDA@Ag@Ag_3PO_4 textiles with visible-light photocatalytic activity were fabricated by reacting the PET@PDA@Ag textiles with $[Ag(NH_3)_2]^+$ complex and Na_2HPO_4 in aqueous solution at room temperature.[40] The existence of Ag not only facilitates the growth of Ag_3PO_4−NPs on the textiles but also promotes visible light absorption and facilitates separation of photo-excited electron−hole pairs.[41] Figure 3a and 3b shows the typical SEM images of the PET@PDA@Ag@Ag_3PO_4 textile. The surface of fibers is inlaid with Ag_3PO_4 submicrocubes which have an average size of 500 nm and a smooth surface. The Ag_3PO_4 submicrocubes are bounded completely by six square {100} facets. Moreover, the characteristic diffraction peaks of both Ag and Ag_3PO_4 can be seen in their XRD patterns (Figure 4a). The diffraction peaks of the Ag_3PO_4

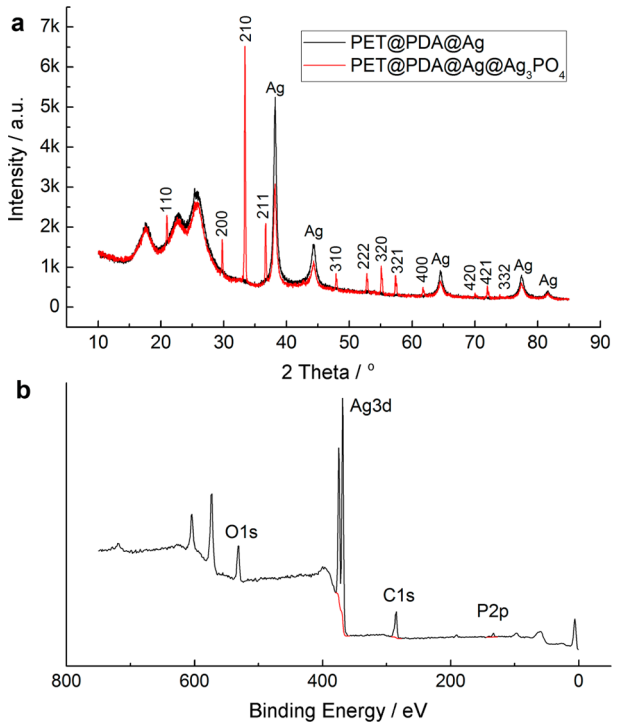

Figure 4. (a) XRD patterns of the PET@PDA@Ag and PET@PDA@Ag@Ag_3PO_4 textiles, and (b) XPS spectrum of the PET@PDA@Ag@Ag_3PO_4 textile.

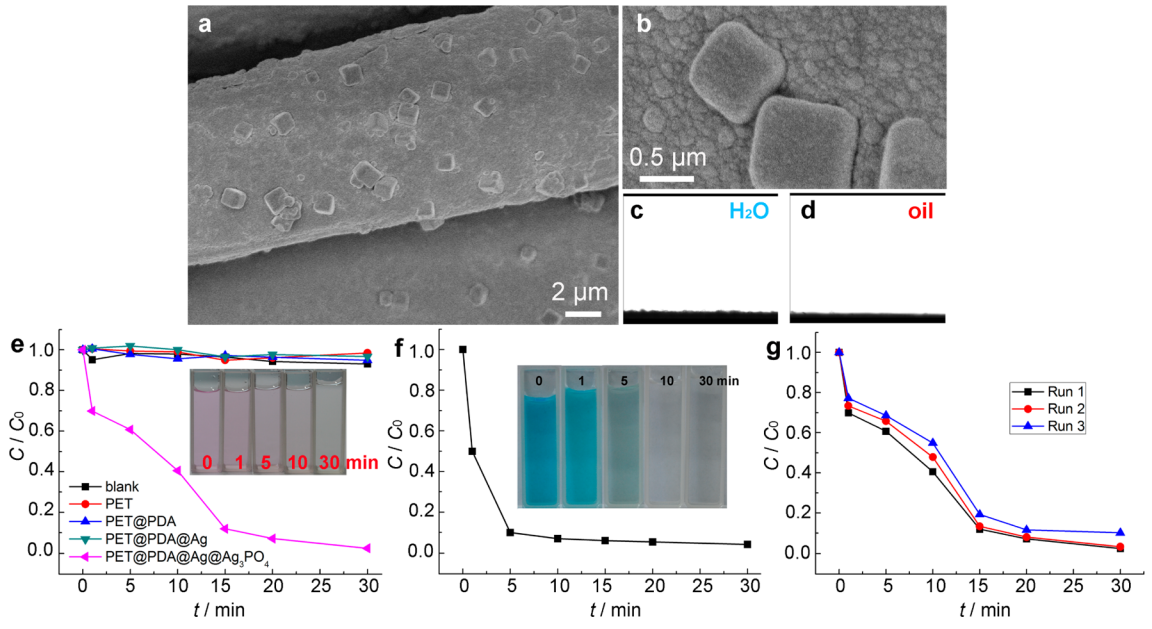

Figure 3. (a and b) SEM images of PET@PDA@Ag@Ag_3PO_4. Images of (c) water and (d) oil drops on PET@PDA@Ag@Ag_3PO_4. Photocatalytic activity of PET@PDA@Ag@Ag_3PO_4 for (e) RhB and (f) MB degradation under visible-light irradiation at $\lambda > 420$ nm, and (g) repeated recycling experiments for RhB degradation. Inserts in e and f show the color changes of the RhB and MB solutions, respectively, corresponding to the irradiation time.

submicrocubes could be primarily indexed to the body-centered cubic structure (JCPDS no. 06-0505). Furthermore, Ag, P, O, and C elements are detected in the XPS spectrum of PET@PDA@Ag@Ag_3PO_4 (Figure 4b), which also indicates that Ag_3PO_4–NPs are formed on the surface.

It is well known that introducing proper surface roughness can change a hydrophobic surface to superhydrophobic or a hydrophilic surface to superhydrophilic.[42,43] Modification of the PET@PDA@Ag textiles with the Ag_3PO_4 submicrocubes results in an evident change in the wettability. The Ag_3PO_4 submicrocubes are hydrophilic, and the rough surface amplifies the hydrophilicity of the textiles. Consequently, the hydrophobic PET@PDA@Ag textiles become superamphiphilic PET@PDA@Ag@Ag_3PO_4 textiles. A surface is termed superamphiphilic if the CAs of both water and oil are below 5°. Water and oil drops could wet and penetrate the PET@PDA@Ag@Ag_3PO_4 textiles in a blink of an eye (Figure 3c and 3d). Only 0.12 s is needed for a water drop to penetrate the PET@PDA@Ag@Ag_3PO_4 textile, which is obviously shorter than the PET@PDA textiles (Movie S1, Supporting Information, part 5). The superamphiphilic property of the PET@PDA@Ag@Ag_3PO_4 textile ensures penetration of both water and oil during oil/water separation. Also, wetting of the PET@PDA@Ag@Ag_3PO_4 textile by water provides a chance for direct interaction between Ag_3PO_4 and water-soluble dyes, which makes the photocatalytic degradation of dyes possible after oil/water separation.

The coexistence of Ag, a good electron acceptor, and Ag_3PO_4 promotes the effective separation of photoexcited electron–hole pairs under visible-light irradiation. The enriched electrons on Ag facilitate their participation in the multiple-electron reduction of oxygen. Meanwhile, the high concentration of holes on Ag_3PO_4 significantly accelerates the rate of photocatalytic degradation of organic dyes.[44] The photocatalytic performance of the PET@PDA@Ag@Ag_3PO_4 textile was evaluated through monitoring the degradation of RhB and MB under visible-light irradiation at $\lambda > 420$ nm. For comparison, the self-degradation of RhB and the performance of other textiles prepared in this study were investigated. Adsorption of dye solution in the dark was also studied. The variation of RhB and MB concentrations with visible-light irradiation time in the degradation experiments are summarized in Figure 3e and 3f, respectively. Self-degradation of RhB in the absence of any photocatalyst is negligible after 30 min. Samples including PET, PET@PDA, and PET@PDA@Ag do not show any photocatalytic activity or absorption for RhB. Adsorption of the PET@PDA@Ag@Ag_3PO_4 textile for RhB (1 ppm) in the dark is about 7% in 30 min (Figure S7, Supporting Information). Unlike the other samples, PET@PDA@Ag@Ag_3PO_4 exhibits excellent photocatalytic activity for the RhB and MB degradation reactions. The PET@PDA@Ag@Ag_3PO_4 textile with a size of 5 × 5 cm could completely degrade 100 mL of RhB (1 ppm) and MB (5 ppm) solutions in 30 min under visible-light irradiation. In addition, the PET@PDA@Ag@Ag_3PO_4 textile can be repeatedly used for photocatalytic degradation of RhB (Figure 3g). The PET@PDA@Ag@Ag_3PO_4 textiles also show excellent photocatalytic activity for degradation of RhB and MB dyes in the sunlight (Figure 5) or even in room conditions (Figure 6). Both RhB and MB can be degraded completely in the sunlight in 5 h. A longer time is needed for the degradation of RhB and MB in room conditions.

Water Purification by DL-PET Textiles. DL-PET textiles are composed of the top superamphiphilic PET@PDA@Ag@Ag_3PO_4 layer and the bottom superhydrophobic/superoleophilic PET@PDA@Ag@DM layer. Thus, water can only wet the top PET@PDA@Ag@Ag_3PO_4 layer, whereas oil can penetrate both layers of the DL-PET textiles. The unique wettability and excellent photocatalytic activity make the DL-PET textiles promising candidates for water purification. DL-PET textiles could not only selectively remove insoluble oils from water but also degrade the soluble dyes in water. The practical water purification experiments were carried out in the simple setup as shown in Figure 7a. The DL-PET textiles were fixed between a glass tube (inner diameter, 25 mm) and a flask.

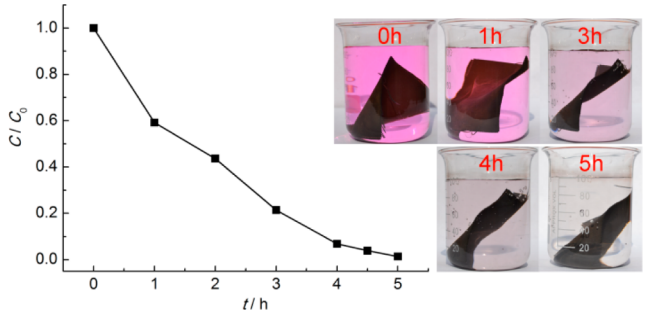

Figure 5. Photocatalytic activity of PET@PDA@Ag@Ag_3PO_4 for RhB (1 ppm) degradation in the sunlight (sunny day, direct sunlight, 30 °C).

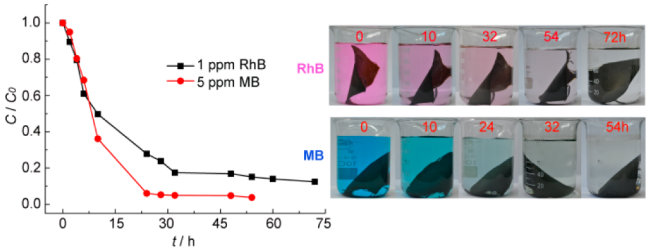

Figure 6. Photocatalytic activity of PET@PDA@Ag@Ag_3PO_4 for RhB (1 ppm) and MB (5 ppm) degradation in room conditions (no direct sunlight, 22 °C).

When the polluted water containing insoluble oil and soluble RhB was poured onto the device, oils with high density will sink to the bottom and penetrate the textile. Oils with low density contact the textile before water when the mixture is slowly pulled into the custom-built setup because of their lower density than water. Meanwhile, water was collected in the glass tube. The water concentration in the collected oil is below 50 ppm, which is in the range of the normal water concentration in *n*-octane. Also, no oil in the collected water can be detected. These results mean very high oil/water separation efficiency of the DL-PET textiles. The top PET@PDA@Ag@Ag_3PO_4 layer was wetted by the RhB aqueous solution after oil/water separation. Subsequently, the RhB dye in water was degraded by the PET@PDA@Ag@Ag_3PO_4 textile under visible-light irradiation. The characteristic peak for RhB at 562 nm completely disappears (Figure 7b). Finally, purified water was obtained after oil/water separation and photocatalytic degradation using the DL-PET textiles.

CONCLUSIONS

In summary, we demonstrated a facile methodology to create multifunctional DL-PET textiles for removal of insoluble oil and soluble dyes in water inspired by the mussel adhesive protein and the lotus leaf. DL-PET textiles are composed of a

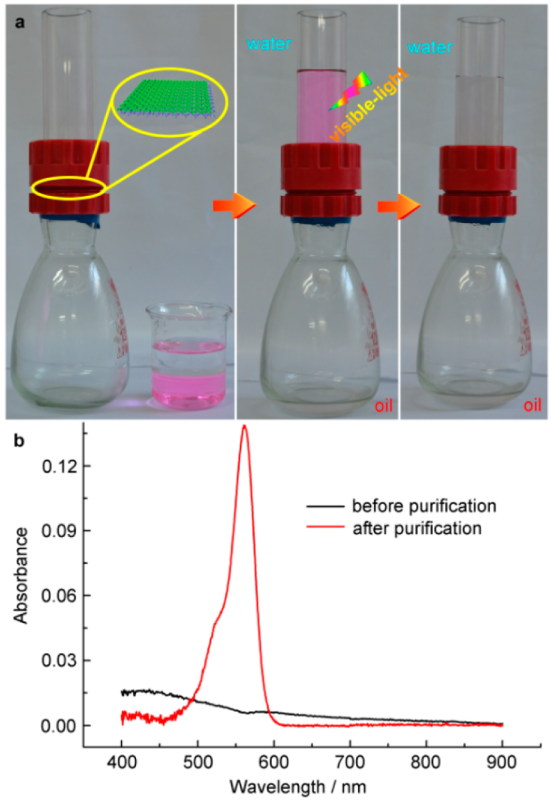

Figure 7. (a) Oil/water separation and visible-light photocatalytic degradation of RhB (1 ppm) using the DL-PET textiles. (b) UV−vis spectra of the 1 ppm RhB aqueous solution and the purified water.

top superamphiphilic layer with immobilized Ag_3PO_4−NPs and a bottom superhydrophobic/superoleophilic layer. The unique wettability of the DL-PET textiles ensures that oil can penetrate both layers of the DL-PET textiles while water can only wet the top layer. The immobilized Ag_3PO_4−NPs on the top layer can then decompose the water-soluble organic contaminants under visible-light irradiation or even the sunlight. The DL-PET textiles feature unique wettability, high oil/water separation efficiency, and visible-light photocatalytic activity. We believe that this study opens the door toward design of multifunctional materials by the combination of bioinspiration, which will have promising applications in many fields, e.g., oil/water separation, wastewater cleaning, and visible-light photocatalysis.

■ ASSOCIATED CONTENT

Ⓢ Supporting Information

Image of a water drop on a superhydrophobic textile, principle setup for measuring WSA, schematic illustration of abrasion tests, digital and SEM images of the samples, and videos. This material is available free of charge via the Internet at http://pubs.acs.org.

■ AUTHOR INFORMATION

Corresponding Author

*E-mail: jpzhang@licp.cas.cn.

Author Contributions

The manuscript was written through contributions of all authors. All authors have given approval to the final version of the manuscript.

Notes

The authors declare no competing financial interest.

■ ACKNOWLEDGMENTS

We are grateful for financial support of the "Hundred Talents Program" of the Chinese Academy of Sciences.

■ REFERENCES

(1) Elliott, J. E.; Elliott, K. H. Tracking Marine Pollution. *Science* **2013**, *340*, 556−558.
(2) de Aragão Umbuzeiro, G.; Freeman, H. S.; Warren, S. H.; De Oliveira, D. P.; Terao, Y.; Watanabe, T.; Claxton, L. D. The Contribution of Azo Dyes to the Mutagenic Activity of the Cristais River. *Chemosphere* **2005**, *60*, 55−64.
(3) Gao, C.; Sun, Z.; Li, K.; Chen, Y.; Cao, Y.; Zhang, S.; Feng, L. Integrated Oil Separation and Water Purification by a Double-Layer TiO_2-Based Mesh. *Energy Environ. Sci.* **2013**, *6*, 1147−1151.
(4) Liu, F.; Chung, S.; Oh, G.; Seo, T. S. Three-Dimensional Graphene Oxide Nanostructure for Fast and Efficient Water-Soluble Dye Removal. *ACS Appl. Mater. Interfaces* **2011**, *4*, 922−927.
(5) Calcagnile, P.; Fragouli, D.; Bayer, I. S.; Anyfantis, G. C.; Martiradonna, L.; Cozzoli, P. D.; Cingolani, R.; Athanassiou, A. Magnetically Driven Floating Foams for the Removal of Oil Contaminants from Water. *ACS Nano* **2012**, *6*, 5413−5419.
(6) Kwon, G.; Kota, A. K.; Li, Y.; Sohani, A.; Mabry, J. M.; Tuteja, A. On-Demand Separation of Oil-Water Mixtures. *Adv. Mater.* **2012**, *24*, 3666−3671.
(7) Bi, Y.; Ouyang, S.; Umezawa, N.; Cao, J.; Ye, J. Facet Effect of Single-Crystalline Ag_3PO_4 Sub-microcrystals on Photocatalytic Properties. *J. Am. Chem. Soc.* **2011**, *133*, 6490−6492.
(8) Wen, Q.; Di, J.; Zhao, Y.; Wang, Y.; Jiang, L.; Yu, J. Flexible Inorganic Nanofibrous Membranes with Hierarchical Porosity for Efficient Water Purification. *Chem. Sci.* **2013**, *4*, 4378−4382.
(9) Zhang, J. P.; Seeger, S. Polyester Materials with Superwetting Silicone Nanofilaments for Oil/Water Separation and Selective Oil Absorption. *Adv. Funct. Mater.* **2011**, *21*, 4699−4704.
(10) Crick, C. R.; Gibbins, J. A.; Parkin, I. P. Superhydrophobic Polymer-coated Copper-mesh; Membranes for Highly Efficient Oil−Water Separation. *J. Mater. Chem. A* **2013**, *1*, 5943−5948.
(11) Yang, J.; Zhang, Z.; Xu, X.; Zhu, X.; Men, X.; Zhou, X. Superhydrophilic-Superoleophobic Coatings. *J. Mater. Chem.* **2012**, *22*, 2834−2837.
(12) Zhu, Q.; Pan, Q.; Liu, F. Facile Removal and Collection of Oils from Water Surfaces through Superhydrophobic and Superoleophilic Sponges. *J. Phys. Chem. C* **2011**, *115*, 17464−17470.
(13) Zhu, Q.; Chu, Y.; Wang, Z.; Chen, N.; Lin, L.; Liu, F.; Pan, Q. Robust Superhydrophobic Polyurethane Sponge as a Highly Reusable Oil-Absorption Material. *J. Mater. Chem. A* **2013**, *1*, 5386−5393.
(14) Gui, X.; Wei, J.; Wang, K.; Cao, A.; Zhu, H.; Jia, Y.; Shu, Q.; Wu, D. Carbon Nanotube Sponges. *Adv. Mater.* **2010**, *22*, 617−621.
(15) Lee, C. H.; Johnson, N.; Drelich, J.; Yap, Y. K. The Performance of Superhydrophobic and Superoleophilic Carbon Nanotube Meshes in Water-Oil Filtration. *Carbon* **2011**, *49*, 669−676.
(16) Hayase, G.; Kanamori, K.; Fukuchi, M.; Kaji, H.; Nakanishi, K. Facile Synthesis of Marshmallow-like Macroporous Gels Usable under Harsh Conditions for the Separation of Oil and Water. *Angew. Chem., Int. Ed.* **2013**, *52*, 1986−1989.
(17) Ono, T.; Sugimoto, T.; Shinkai, S.; Sada, K. Lipophilic Polyelectrolyte Gels as Super-Absorbent Polymers for Nonpolar Organic Solvents. *Nat. Mater.* **2007**, *6*, 429−433.
(18) Zhang, Y.; Wei, S.; Liu, F.; Du, Y.; Liu, S.; Ji, Y.; Yokoi, T.; Tatsumi, T.; Xiao, F. S. Superhydrophobic Nanoporous Polymers as Efficient Adsorbents for Organic Compounds. *Nano Today* **2009**, *4*, 135−142.
(19) Zhang, X. Y.; Li, Z.; Liu, K. S.; Jiang, L. Bioinspired Multifunctional Foam with Self-Cleaning and Oil/Water Separation. *Adv. Funct. Mater.* **2013**, *23*, 2881−2886.
(20) Li, A.; Sun, H. X.; Tan, D. Z.; Fan, W. J.; Wen, S. H.; Qing, X. J.; Li, G. X.; Li, S. Y.; Deng, W. Q. Superhydrophobic Conjugated Microporous Polymers for Separation and Adsorption. *Energy Environ. Sci.* **2011**, *4*, 2062−2065.

(21) Sun, H.; Li, A.; Zhu, Z.; Liang, W.; Zhao, X.; La, P.; Deng, W. Superhydrophobic Activated Carbon-Coated Sponges for Separation and Absorption. *ChemSusChem* **2013**, *6*, 1057−1062.
(22) Kota, A. K.; Kwon, G.; Choi, W.; Mabry, J. M.; Tuteja, A. Hygro-Responsive Membranes for Effective Oil−Water Separation. *Nat. Commun.* **2012**, *3*, 1025.
(23) Jin, M.; Wang, J.; Yao, X.; Liao, M.; Zhao, Y.; Jiang, L. Underwater Oil Capture by a Three-Dimensional Network Architectured Organosilane Surface. *Adv. Mater.* **2011**, *23*, 2861−2864.
(24) Xue, Z.; Wang, S.; Lin, L.; Chen, L.; Liu, M.; Feng, L.; Jiang, L. A Novel Superhydrophilic and Underwater Superoleophobic Hydrogel-Coated Mesh for Oil/Water Separation. *Adv. Mater.* **2011**, *23*, 4270−4273.
(25) Li, K.; Ju, J.; Xue, Z.; Ma, J.; Feng, L.; Gao, S.; Jiang, L. Structured Cone Arrays for Ccontinuous and Effective Collection of Micron-Sized Oil Droplets from Water. *Nat. Commun.* **2013**, *4*, 2276.
(26) Yi, Z.; Ye, J.; Kikugawa, N.; Kako, T.; Ouyang, S.; Stuart-Williams, H.; Yang, H.; Cao, J.; Luo, W.; Li, Z.; Liu, Y.; Withers, R. L. An Orthophosphate Semiconductor with Photooxidation Properties under Visible-Light Irradiation. *Nat. Mater.* **2010**, *9*, 559−564.
(27) Reijnders, L. Hazard Reduction for the Application of Titania Nanoparticles in Environmental Technology. *J. Hazard. Mater.* **2008**, *152*, 440−445.
(28) Meseck, G. R.; Kontic, R.; Patzke, G. R.; Seeger, S. Photocatalytic Composites of Silicone Nanofilaments and TiO2 Nanoparticles. *Adv. Funct. Mater.* **2012**, *22*, 4433−4438.
(29) Zimmermann, J.; Reifler, F. A.; Fortunato, G.; Gerhardt, L. C.; Seeger, S. A Simple, One-Step Approach to Durable and Robust Superhydrophobic Textiles. *Adv. Funct. Mater.* **2008**, *18*, 3662−3669.
(30) Zimmermann, J.; Seeger, S.; Reifler, F. A. Water Shedding Angle: A New Technique to Evaluate the Water-Repellent Properties of Superhydrophobic Surfaces. *Text. Res. J.* **2009**, *79*, 1565−1570.
(31) Zhu, X.; Zhang, Z.; Yang, J.; Xu, X.; Men, X.; Zhou, X. Facile Fabrication of a Superhydrophobic Fabric with Mechanical Stability and Easy-Repairability. *J. Colloid Interface Sci.* **2012**, *380*, 182−186.
(32) Lee, H.; Dellatore, S. M.; Miller, W. M.; Messersmith, P. B. Mussel-Inspired Surface Chemistry for Multifunctional Coatings. *Science* **2007**, *318*, 426−430.
(33) Zhang, L.; Wu, J.; Wang, Y.; Long, Y.; Zhao, N.; Xu, J. Combination of Bioinspiration: A General Route to Superhydrophobic Particles. *J. Am. Chem. Soc.* **2012**, *134*, 9879−9881.
(34) Kim, K.; Kim, H. S.; Park, H. K. Facile Method to Prepare Surface-Enhanced-Raman-Scattering-Active Ag Nanostructures on Silica Spheres. *Langmuir* **2006**, *22*, 8083−8088.
(35) Lee, D. J.; Kim, H. M.; Song, Y. S.; Youn, J. R. Water Droplet Bouncing and Superhydrophobicity Induced by Multiscale Hierarchical Nanostructures. *ACS Nano* **2012**, *6*, 7656−7664.
(36) Deng, B.; Cai, R.; Yu, Y.; Jiang, H.; Wang, C.; Li, J.; Li, L.; Yu, M.; Li, J.; Xie, L. Laundering Durability of Superhydrophobic Cotton Fabric. *Adv. Mater.* **2010**, *22*, 5473−5477.
(37) Gao, Q.; Zhu, Q.; Guo, Y.; Yang, C. Q. Formation of Highly Hydrophobic Surfaces on Cotton and Polyester Fabrics Using Silica Sol Nanoparticles and Nonfluorinated Alkylsilane. *Ind. Eng. Chem. Res.* **2009**, *48*, 9797−9803.
(38) Crick, C. R.; Parkin, I. P. Water Droplet Bouncing-A Definition for Superhydrophobic Surfaces. *Chem. Commun.* **2011**, *47*, 12059−12061.
(39) Zhang, J.; Li, B.; Wu, L.; Wang, A. Facile Preparation of Durable and Robust Superhydrophobic Textiles by Dip Coating in Nanocomposite Solution of Organosilanes. *Chem. Commun.* **2013**, *49*, 11509−11511.
(40) Bi, Y.; Hu, H.; Ouyang, S.; Jiao, Z.; Lu, G.; Ye, J. Selective Growth of Ag_3PO_4 Submicro-Cubes on Ag Nanowires to Fabricate Necklace-Like Heterostructures for Photocatalytic Applications. *J. Mater. Chem.* **2012**, *22*, 14847−14850.
(41) Lin, Y.; Hsu, Y.; Chen, Y.; Wang, S.; Miller, J.; Chen, L.; Chen, K. Plasmonic $Ag@Ag_3(PO_4)_{1-x}$ Nanoparticle Photosensitized ZnO Nanorod-array Photoanodes for Water Oxidation. *Energy Environ. Sci.* **2012**, *5*, 8917−8922.
(42) Zhang, J.; Seeger, S. Silica/Silicone Nanofilament Hybrid Coatings with Almost Perfect Superhydrophobicity. *ChemPhysChem* **2013**, *14*, 1646−1651.
(43) Wu, L.; Zhang, J.; Li, B.; Wang, A. Mimic Nature, Beyond Nature: Facile Synthesis of Durable Superhydrophobic Textiles Using Organosilanes. *J. Mater. Chem. B* **2013**, *1*, 4756−4763.
(44) Hu, H. Y.; Jiao, Z. B.; Wang, T.; Ye, J. H.; Lu, G. X.; Bi, Y. P. Enhanced Photocatalytic Activity of Ag/Ag_3PO_4 Coaxial Heteronanowires. *J. Mater. Chem. A* **2013**, *1*, 10612−10616.